

Carbohydrate-Appended 2,2'-Dipicolylamine Metal Complexes as Potential Imaging Agents

Tim Storr,[†] Yuko Sugai,[‡] Cheri A. Barta,[†] Yuji Mikata,[‡] Michael J. Adam,^{*,§} Shigenobu Yano,^{||} and Chris Orvig^{*,†}

Department of Chemistry, University of British Columbia, 2036 Main Mall, Vancouver, British Columbia V6T 1Z1, Canada, KYOUSEI Science Center, Nara 630-8506, Japan, TRIUMF, 4004 Wesbrook Mall, Vancouver, British Columbia V6T 2A3, Canada, and Division of Material Science, Nara 630-8506, Japan

Received October 19, 2004

Three discrete carbohydrate-appended 2,2'-dipicolylamine ligands were complexed to the $\{M(\text{CO})_3\}^+$ ($M = {}^{99m}\text{Tc}/\text{Re}$) core: 2-(bis(2-pyridinylmethyl)amino)ethyl- β -D-glucopyranoside (L^1), 2-(bis(2-pyridinylmethyl)amino)ethyl- β -D-xylopyranoside (L^2), and 2-(bis(2-pyridinylmethyl)amino)ethyl- α -D-mannopyranoside (L^3). An ethylene spacer is used to separate the carbohydrate moiety and the dipicolylamine (DPA) function in all three ligands. The Re complexes $[\text{Re}(\text{L}^{1-3})(\text{CO})_3]\text{Br}$ were characterized by ^1H and ^{13}C 1D/2D NMR spectroscopies, which confirmed the pendant nature of the carbohydrate moieties in solution. NMR measurements also established the long-range asymmetric effect of the carbohydrate functions on the chelating portion of the ligand. One analogue, $[\text{Re}(\text{L}^1)(\text{CO})_3]\text{Cl}$, was characterized in the solid state by X-ray crystallography. Further characterization was provided by IR spectroscopy, elemental analysis, conductivity, and mass spectrometry. Radiolabeling of L^1 – L^3 with $[{}^{99m}\text{Tc}(\text{H}_2\text{O})_3(\text{CO})_3]^+$ afforded high yield compounds of identical character to the Re analogues. The radiolabeled compounds were found to be stable toward ligand exchange in the presence of a large excess of either cysteine or histidine over a 24-h period.

Introduction

The recent interest in the development of radiopharmaceuticals utilizing the group VII metals is a direct result of the ideal properties of ${}^{99m}\text{Tc}$ and ${}^{186/188}\text{Re}$ for diagnosis and therapy, respectively.¹ ${}^{99m}\text{Tc}$ is the most commonly used isotope in single-photon emission-computed tomography (SPECT) due to its ideal nuclear properties ($t_{1/2} = 6.01$ h, $\gamma = 142.7$ keV) and easy isolation as $\text{Na}{}^{99m}\text{TcO}_4$ from a ${}^{99}\text{Mo}$ generator. Rhenium, the third row transition metal analogue of technetium, exhibits chemistry similar to that of technetium and has particle-emitting radioisotopes (${}^{186}\text{Re}$ $t_{1/2} = 3.68$ days, $\beta = 1.07$ MeV, $\gamma = 137$ keV; ${}^{188}\text{Re}$ $t_{1/2} = 16.98$ h, $\beta = 2.12$ MeV, $\gamma = 155$ keV) with physical properties

applicable to therapeutic nuclear medicine. The possibility of designing radiopharmaceuticals for diagnosis (${}^{99m}\text{Tc}$) and therapy (${}^{186/188}\text{Re}$) by exploiting the similar chemistry of these two group VII metals is thus a highly desirable goal in areas such as tumor imaging and therapy.

One compound that has proven very useful for the detection of tumors and metastatic tissue is 2-deoxy-2- $[{}^{18}\text{F}]$ -fluoro-D-glucose (FDG) (Chart 1), imaged by positron emission tomography (PET).² Because the production of ${}^{18}\text{F}$ requires a cyclotron and the isotope has a short (110 min) half-life, its utility is somewhat limited as compared to that of single-photon emitters in nuclear medicine. We have thus endeavored to design carbohydrate-appended Re and Tc complexes for potential use in nuclear medicine.^{3–5} Our

* Authors to whom correspondence should be addressed. E-mail: adam@triumf.ca (M.J.A.); orvig@chem.ubc.ca (C.O.).

[†] University of British Columbia.

[‡] KYOUSEI Science Center.

[§] TRIUMF.

^{||} Division of Material Science.

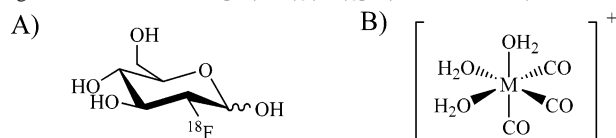
(1) (a) Nicolini, M.; Bandoli, G.; Mazzi, U. *Technetium, Rhenium and Other Metals in Chemistry and Nuclear Medicine*, 5; Raven Press: New York, 2000. (b) Liu, S. *Chem. Soc. Rev.* **2004**, *33*, 445–461. (c) Jurisson, S. S.; Lydon, J. D. *Chem. Rev.* **1999**, *99*, 2205–2218.

(2) Fowler, J. S.; Wolf, A. P. *Acc. Chem. Res.* **1997**, *30*, 181–188.

(3) Bayly, S. R.; Fisher, C. L.; Storr, T.; Adam, M. J.; Orvig, C. *Bioconjugate Chem.* **2004**, *15*, 923–926.

(4) Storr, T.; Obata, M.; Fisher, C. L.; Bayly, S. R.; Green, D. E.; Brudzinska, I.; Mikata, Y.; Patrick, B. O.; Adam, M. J.; Yano, S.; Orvig, C. *Chem. Eur. J.* **2005**, *11*, 195–203.

(5) Storr, T.; Fisher, C. L.; Mikata, Y.; Yano, S.; Adam, M. J.; Orvig, C. *J. Chem. Soc., Dalton Trans.* **2005**, 654–655.

Chart 1. (A) 2-Deoxy-2-[^{18}F]fluoro-D-glucose (FDG); (B) the Organometallic Precursor $[\text{M}(\text{H}_2\text{O})_3(\text{CO})_3]^+$ ($\text{M} = \text{Re}, ^{99m}\text{Tc}$)

approach is to attach a chelating ligand to a carbohydrate that, in a subsequent reaction, will bind to the metal center. This approach is necessary in order to minimize the effects of the tracer group and provide a stable and easily characterized complex. Direct metal ion–carbohydrate interactions are difficult to study due to their inherent multifunctionality, complicated stereochemistry, and weak coordinating ability. Carbohydrate ligands with well-tailored binding groups for metal ions have previously been developed in order to overcome these difficulties. Designed binding groups include iminodiacetic acid,^{6,7} tris(2-aminoethyl)amine,⁸ 1,4,7-triazacyclononane,⁹ imino¹⁰ and amino³ phenols, ethylenediamine,^{11,12} 1,3-propanediamine,^{12,13} and ethylenedicycysteine.¹⁴ Examples of this approach in medicinal inorganic chemistry include carbohydrate-appended *cis*-platin analogues as potent antitumor agents,^{13,15} antifungal Ni(II) complexes derived from amino sugars,¹⁶ and carbohydrate-appended metal complexes of the radioisotopes ^{99m}Tc and ^{186}Re for potential use in nuclear imaging and therapy.^{3–6,14} In many cases however the resultant metal complexes exhibit binding of the carbohydrate moiety to the metal center, which limits the targeting potential of these compounds.

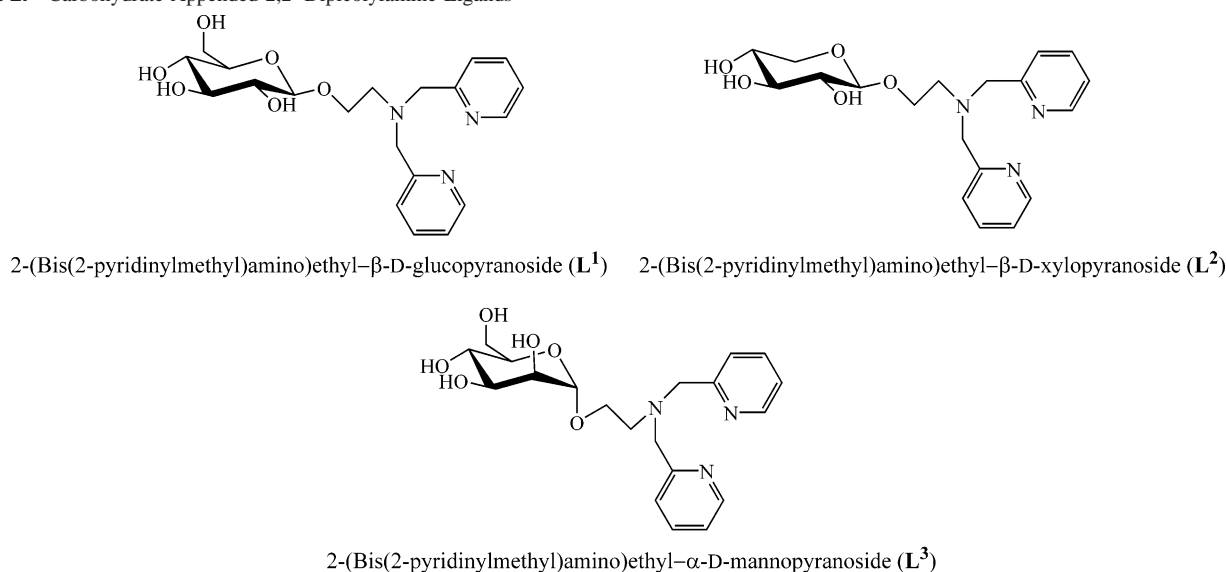
Tc carbohydrate conjugates have not been extensively studied in the literature, with early work, typical of metal–carbohydrate chemistry, plagued by poor characterization as well as potential interactions/chelation of the carbohydrate

itself with the metal center.¹⁷ Factors that most likely effect recognition *in vivo* include the size of the metal chelate as well as the distance between the chelate and the pendant carbohydrate moiety. One recent study utilizing ethylenedicycysteine–deoxyglucose (ECDG) as the chelate for ^{99m}Tc displayed hexokinase activity as well as tumor uptake.¹⁴ Further studies have shown that this compound is active in the hexosamine biosynthetic pathway and has significant *in vivo* tumor imaging potential.¹⁸ Uptake in tumor cells has also been demonstrated for the ^{99m}Tc complex of 1,3-*N,N*-di- β -D-glucopyranosyldiethylenetriamine (DGTA), even in the presence of excess glucose in the culture medium.¹⁹ Both studies highlight the potential of carbohydrate-labeled ^{99m}Tc compounds for tumor imaging.

Stable core structures have found utility in the chemistry of Tc due to the wide range of accessible oxidation states [Tc(–I) to Tc(VII)]. For example, the $\{\text{M}(\text{CO})_3\}^+$ ($\text{M} = \text{Tc}/\text{Re}$) (Chart 1) core has garnered significant interest ever since its development by Jaouen²⁰ and Alberto²¹ and co-workers. This organometallic core offers advantages in terms of stability, kinetic inertness, and size. The low-spin d^6 -electron configuration and the stability of the CO ligands to substitution further protect the metal center from ligand substitution and/or oxidation. For the above reasons there has been widespread interest in the development of target-specific radiopharmaceuticals utilizing the $\{\text{M}(\text{CO})_3\}^+$ (Tc/Re) core.²²

The labeling precursor $[\text{M}(\text{H}_2\text{O})_3(\text{CO})_3]^+$ (Chart 1) is easily prepared from a kit formulation in aqueous conditions utilizing a boranocarbonate as a dual-function reducing agent

- (6) Petrig, J.; Schibli, R.; Dumas, C.; Alberto, R.; Schubiger, P. A. *Chem. Eur. J.* **2001**, *7*, 1868–1873.
- (7) Dumas, C.; Schibli, R.; Schubiger, P. A. *J. Org. Chem.* **2003**, *68*, 512–518.
- (8) (a) Tanase, T.; Doi, M.; Nouchi, R.; Kato, M.; Sato, Y.; Ishida, K.; Kobayashi, K.; Sakurai, T.; Yamamoto, Y.; Yano, S. *Inorg. Chem.* **1996**, *35*, 4848–4857. (b) Tanase, T.; Onaka, T.; Nakagoshi, M.; Kinoshita, I.; Shibata, K.; Doe, M.; Fujii, J.; Yano, S. *Inorg. Chem.* **1999**, *38*, 3150–3159.
- (9) Tanase, T.; Inukai, H.; Onaka, T.; Kato, M.; Yano, S.; Lippard, S. J. *Inorg. Chem.* **2001**, *40*, 3943–3953.
- (10) Adam, M. J.; Hall, L. D. *Can. J. Chem.* **1982**, *60*, 2229–2237.
- (11) Mikata, Y.; Yoneda, K.; Tanase, T.; Kinoshita, I.; Doe, M.; Nishida, F.; Mochida, K.; Yano, S. *Carbohydr. Res.* **1998**, *313*, 175–179.
- (12) Mikata, Y.; Shinohara, Y.; Yoneda, K.; Nakamura, Y.; Esaki, K.; Tanahashi, M.; Brudzinska, I.; Hirohara, S.; Yokoyama, M.; Mogami, K.; Tanase, T.; Kitayama, T.; Takashiba, K.; Nabeshima, K.; Takagi, R.; Takatani, M.; Okamoto, T.; Kinoshita, I.; Doe, M.; Hamazawa, A.; Morita, M.; Nishida, F.; Sakakibara, T.; Orvig, C.; Yano, S. *J. Org. Chem.* **2001**, *66*, 3783–3789.
- (13) Chen, Y. S.; Heeg, M. J.; Brauschweiger, P. G.; Xie, W. H.; Wang, P. G. *Angew. Chem., Int. Ed.* **1999**, *38*, 1768–1769.
- (14) Yang, D. J.; Kim, C. G.; Schechter, N. R.; Azhdarinia, A.; Yu, D. F.; Oh, C. S.; Bryant, J. L.; Won, J. J.; Kim, E. E.; Podoloff, D. A. *Radiology* **2003**, *226*, 465–473.
- (15) (a) Mikata, Y.; Shinohara, Y.; Yoneda, K.; Nakamura, Y.; Brudzinska, I.; Tanase, T.; Kitayama, T.; Takagi, R.; Okamoto, T.; Kinoshita, I.; Doe, M.; Orvig, C.; Yano, S. *Bioorg. Med. Chem. Lett.* **2001**, *11*, 3045–3047. (b) Tsubomura, T.; Ogawa, M.; Yano, S.; Kobayashi, K.; Sakurai, T.; Yoshikawa, S. *Inorg. Chem.* **1990**, *29*, 2622–2626.
- (16) Yano, S.; Inoue, S.; Nouchi, R.; Mogami, K.; Shinohara, Y.; Yasuda, Y.; Kato, M.; Tanase, T.; Kakuchi, T.; Mikata, Y.; Suzuki, T.; Yamamoto, Y., *J. Inorg. Biochem.* **1998**, *69*, 15–23.
- (17) (a) Ozker, K.; Collier, B. D.; Lindner, D. J.; Kabasakal, L.; Liu, Y.; Krasnow, A. Z.; Hellman, R. S.; Edwards, S. D.; Bourque, C. R.; Crane, P. D. *Nucl. Med. Commun.* **1999**, *20*, 1055–1058. (b) Caner, B. E.; Ercan, M. T.; Bekdik, C. F.; Varoglu, E.; Muezzinoglu, S.; Duman, Y.; Erbenli, G. F. *Nuklearmedizin* **1991**, *30*, 132–136. (c) Risch, V. R.; Honda, T.; Heindel, N. D.; Emrich, J. L.; Brady, L. W. *Radiology* **1977**, *124*, 837–838. (d) Wang, T. S. T.; Hosain, P.; Spencer, R. P.; Hosain, F. *Nuklearmedizin* **1977**, *16*, 89–90.
- (18) Rollo, F. D.; Bryant, J.; Yang, D. J.; Bai, C.; Kim, E. E.; Yu, D. F.; Ye, J.; Da Silva, A. J.; Durbin, M. K.; Garrard, J.; Shao, L. *51st Society for Nuclear Medicine Annual Meeting*; 2004; 336P (Abstract 1062).
- (19) Kim, Y.; Kang, S. H.; Oh, S. J.; Ryu, J. S.; Kim, J. S.; Yeo, J. S.; Choi, S. J.; Park, K. B.; Moon, D. H. *51st Society for Nuclear Medicine Annual Meeting*; 2004; 458P (Abstract 1425).
- (20) Top, S.; Elhafa, H.; Vessieres, A.; Quivy, J.; Vaissermann, J.; Hughes, D. W.; McGlinchey, M. J.; Mornon, J. P.; Thoreau, E.; Jaouen, G. *J. Am. Chem. Soc.* **1995**, *117*, 8372–8380.
- (21) Alberto, R.; Schibli, R.; Waibel, R.; Abram, U.; Schubiger, A. P. *Coord. Chem. Rev.* **1999**, *192*, 901–919.
- (22) (a) Zobi, F.; Spingler, B.; Fox, T.; Alberto, R. *Inorg. Chem.* **2003**, *42*, 2818–2820. (b) Waibel, R.; Alberto, R.; Willuda, J.; Finern, R.; Schibli, R.; Stichelberger, A.; Egli, A.; Abram, U.; Mach, J. P.; Pluckthun, A.; Schubiger, P. A. *Nat. Biotechnol.* **1999**, *17*, 897–901. (c) Spradua, T. W.; Katzenellenbogen, J. A. *Bioorg. Med. Chem. Lett.* **1998**, *8*, 3235–3240. (d) Smith, C. J.; Sieckman, G. L.; Owen, N. K.; Hayes, D. L.; Mazuru, D. G.; Kannan, R.; Volkert, W. A.; Hoffman, T. J. *Cancer Res.* **2003**, *63*, 4082–4088. (e) Skadden, M. B.; Wust, F. R.; Jonson, S.; Syhre, R.; Welch, M. J.; Spies, H.; Katzenellenbogen, J. A. *Nucl. Med. Biol.* **2000**, *27*, 269–278. (f) Lee, B. C.; Choe, Y. S.; Chi, D. Y.; Paik, J. Y.; Lee, K. H.; Choi, Y.; Kim, B. T. *Bioconjugate Chem.* **2004**, *15*, 121–127. (g) La Bella, R.; Garcia-Garayoa, E.; Bahler, M.; Blauenstein, P.; Schibli, R.; Conrath, P.; Tourwe, D.; Schubiger, P. A. *Bioconjugate Chem.* **2002**, *13*, 599–604. (h) La Bella, R.; Garcia-Garayoa, E.; Langer, M.; Blauenstein, P.; Beck-Sickinger, A. G.; Schubiger, P. A. *Nucl. Med. Biol.* **2002**, *29*, 553–560. (i) Jaouen, G.; Top, S.; Vessieres, A.; Pigeon, P.; Leclercq, G.; Laios, I. *Chem. Commun.* **2001**, 383–384. (j) Amann, A.; Decristoforo, C.; Ott, I.; Wenger, M.; Bader, D.; Alberto, R.; Putz, G. *Nucl. Med. Biol.* **2001**, *28*, 243–250.

Chart 2. Carbohydrate-Appended 2,2'-Dipyridylamine Ligands

and in situ CO source.²³ The three labile water molecules are readily exchanged for suitable chelating ligands in a facial arrangement. Previous work has found that a tridentate approach utilizing aromatic or aliphatic amines is the best match for the $\{M(\text{CO})_3\}^+$ (Tc/Re) core.^{24–26} Complexes of bidentate ligands with $\{^{99\text{m}}\text{Tc}(\text{CO})_3\}^+$, while exhibiting moderate stability toward ligand exchange, were found to exhibit poor clearance due to plasma protein binding, most likely through the free coordination site on the metal center.²⁴ To design robust carbohydrate-appended metal complexes of Tc and Re with better pharmacokinetic profiles, the DPA function was chosen as the binding group. This tridentate chelator (containing two pyridines and one tertiary amine) avidly binds the $\{\text{Re}(\text{CO})_3\}^+$ core;²⁵ more recently, this chelate system has been used to attach $\{\text{Re}(\text{CO})_3\}^+$ as a proof of principle for the preparation of peptide-targeted radiopharmaceuticals,²⁷ and to prepare molecules to monitor dopamine transporter sites,²⁸ and to image the hepatobiliary system.²⁹ An initial study by Mikata et al.³⁰ concerning the synthesis and characterization of a glucose-pendant DPA copper complex shows the utility of this approach for the carbohydrate labeling of metal ions.

In an effort to develop carbohydrate-appended imaging agents, we have investigated the utility of carbohydrate-

appended DPA conjugates (Chart 2) as ligands for the $\{M(\text{CO})_3\}^+$ ($^{99\text{m}}\text{Tc}/\text{Re}$) core. In all cases the carbohydrate moiety is connected to the chelating unit via the C-1 position. Structural investigations were initially carried out on the “cold” Re derivatives utilizing the starting material $[\text{NEt}_4]_2\text{-}[\text{ReBr}_3(\text{CO})_3]^{31}$ to ascertain solution and solid-state configuration. In solution, the compounds were analyzed by 1D ($^1\text{H}/^{13}\text{C}$) as well as by 2D ($^1\text{H}-^1\text{H}$ COSY and $^1\text{H}-^{13}\text{C}$ HMQC) NMR experiments. Solution structure was further probed by mass spectrometry and conductivity. One analogue $[\text{Re}(\text{L}^1)(\text{CO})_3]\text{Cl}$ was analyzed by X-ray crystallography. Labeling studies and preliminary in vitro stability measurements for the analogous $^{99\text{m}}\text{Tc}$ derivatives are also presented.

Experimental Section

General Methods. All solvents and chemicals (Fisher, Aldrich) were reagent grade and used without further purification unless otherwise specified. Ligand **L¹**³⁰ and $[\text{NEt}_4]_2[\text{Re}(\text{CO})_3\text{Br}_3]^{31}$ were synthesized according to previously published procedures. **L²** and **L³** were synthesized in a fashion similar to **L¹** with details to be published elsewhere.³² ^1H and ^{13}C NMR spectra were recorded on a AV-400 instrument at 400.13 (100.62 for ^{13}C NMR spectra) MHz. Infrared spectra were recorded as thin films on an AgBr plate in the range of 4000–400 cm^{-1} on a Galaxy series FTIR spectrometer. Mass spectra (positive ion) were obtained on dilute MeOH solutions using a Macromass LCT (electrospray ionization) instrument. C, H, N analyses were performed at the University of British Columbia by Mr. M. Lakha (Carlo Erba analytical instrumentation). Conductivity measurements were performed using a Serfass conductance bridge model RCM151B (Arthur Thomas Co. Ltd.) connected to a 3403 cell (Yellow Springs Instrument Co.). The cell was calibrated using a 0.01000 M KCl solution with a molar conductance (Λ_m) of 141.3 $\Omega^{-1}\text{cm}^2\text{mol}^{-1}$ at 25 °C to determine the cell constant to be 1.016 cm^{-1} .³³ Solutions were prepared at 1 mM.

(23) Alberto, R.; Ortner, K.; Wheatley, N.; Schibli, R.; Schubiger, P. A. *J. Am. Chem. Soc.* **2001**, *123*, 3135–3136.

(24) Schibli, R.; La Bella, R.; Alberto, R.; Garcia-Garayoa, E.; Ortner, K.; Abram, U.; Schubiger, P. A. *Bioconjugate Chem.* **2000**, *11*, 345–351.

(25) Banerjee, S. R.; Levadala, M. K.; Lazarova, N.; Wei, L. H.; Valliant, J. F.; Stephenson, K. A.; Babich, J. W.; Maresca, K. P.; Zubieta, J. *Inorg. Chem.* **2002**, *41*, 6417–6425.

(26) Rattat, D.; Eraets, K.; Cleyhens, B.; Knight, H.; Fonge, H.; Verbruggen, A. *Tetrahedron Lett.* **2004**, *45*, 2531–2534.

(27) Stephenson, K. A.; Zubieta, J.; Banerjee, S. R.; Levadala, M. K.; Taggart, L.; Ryan, L.; McFarlane, N.; Boreham, D. R.; Maresca, K. P.; Babich, J. W.; Valliant, J. F. *Bioconjugate Chem.* **2004**, *15*, 128–136.

(28) Wei, L. H.; Banerjee, S. R.; Levadala, M. K.; Babich, J.; Zubieta, J. *Inorg. Chim. Acta* **2004**, *357*, 1499–1516.

(29) Liu, G.; Dou, S.; He, J.; Vanderheyden, J.; Ruszkowski, M.; Hnatowich, D. J. *Bioconjugate Chem.* **2004**, *15*, 1441–1446.

(30) Mikata, Y.; Sugai, Y.; Yano, S. *Inorg. Chem.* **2004**, *43*, 4778–4780.

(31) Alberto, R.; Egli, A.; Abram, U.; Hegetschweiler, K.; Gramlich, V.; Schubiger, P. A. *J. Chem. Soc., Dalton Trans.* **1994**, 2815–2820.

(32) Mikata, Y.; Sugai, Y. Unpublished results.

(33) (a) Geary, W. J. *Coord. Chem. Rev.* **1971**, *7*, 81–122. (b) Huheey, J. E. *Inorganic Chemistry: Principles of Structure and Reactivity*, 3rd ed.; Harper Collins Publishers: New York, 1983; p 362.

Table 1. Selected Crystal Data for the Structure of [Re(L¹)(CO)₃]Cl

formula	C ₂₆ H ₃₆ ClN ₃ O _{10.5} Re	β, deg	90
fw	780.23	γ, deg	90
space group	P2 ₁ 2 ₁ 2	V, Å ³	3053.8(8)
T, K	173(2)	Z	4
a, Å	36.523(6)	D _{calc} , g cm ⁻³	1.697
b, Å	8.2197(11)	μ, mm ⁻¹	7.1073
c, Å	10.1723(16)	R1 ^a [I > 2θ(I)]	0.0219
α, deg	90	wR2 ^b	0.0508

$$^a R1 = \sum ||F_o| - |F_c|| / \sum |F_o|. \quad ^b wR2 = [\sum w(F_o^2 - F_c^2)^2 / \sum w(F_o^2)]^{1/2}.$$

X-ray Crystallography. Colorless crystals of [Re(L¹)(CO)₃]Cl·Et₂O·MeOH were obtained via slow vapor diffusion of diethyl ether into a concentrated methanol solution of the Re compound containing excess NaCl. The crystals were mounted on a glass fiber and cooled to -100.0 ± 0.1 °C, and data were collected on a Bruker X8 APEX diffractometer using graphite-monochromated Mo Kα radiation ($\lambda = 0.71073$ Å) to a maximum 2θ value of 56.0°. Data were collected and integrated using the Bruker SAINT³⁴ software package and corrected for Lorentz and polarization effects as well as absorption (SADABS³⁵). The structure was solved by direct methods (SIR92³⁶) with all non-hydrogen atoms refined anisotropically. Hydrogen atoms were added but not refined. The final refinement was completed using SHELXL-97.³⁷ The maximum and minimum peaks in the final differential Fourier map were 1.470 and -0.576 e⁻/Å⁻³. The relevant parameters for crystal data, structure solution, and refinement are summarized in Table 1. The CIF file is available in the Supporting Information.

^{99m}Tc(H₂O)₃(CO)₃]⁺ Labeling Studies. The organometallic precursor [^{99m}Tc(H₂O)₃(CO)₃]⁺ was prepared from a saline solution of Na[^{99m}TcO₄] (1 mL, 200 MBq) using an Isolink kit provided by Mallinckrodt Inc. Briefly, a 1 mL solution of Na[^{99m}TcO₄] was added to an Isolink kit, and the vial was heated to reflux for 20 min. Upon cooling, 1 mL of a 0.1 M HCl solution was added to adjust the pH to 9–10. Labeling was achieved by mixing an aliquot (200 μL) of the [^{99m}Tc(H₂O)₃(CO)₃]⁺ precursor with a 0.1 mM solution of L¹–L³ or histidine in PBS (pH 7.4, 1 mL) and incubating at 75 °C for 30 min. HPLC analyses were performed on a Knauer Wellchrom K-1001 HPLC equipped with a K-2501 absorption detector and a Capintek radiometric well counter. A Synergi 4 μm C-18 Hydro-RP analytical column with dimensions of 250 × 4.6 mm was used. HPLC solvents consisted of 0.1% trifluoroacetic acid in water (solvent A) and acetonitrile (solvent B). Samples were analyzed with a linear gradient method (100% solvent A to 100% solvent B over 30 min).

Cysteine and Histidine Challenge Experiments. To a 900 μL solution of either cysteine or histidine in PBS (1 mM, pH = 7.4) was added a solution of the ^{99m}Tc complex (final ligand concentration 10⁻⁵ M). The samples were incubated at 37 °C, and aliquots were removed at 1, 4, and 24 h for analysis by HPLC.

(2-Bis(2-pyridinylmethyl)amino)ethyl-β-D-glucopyranosyl)-tricarboxylrhodium bromide [Re(L¹)(CO)₃]Br. A solution of [NEt₄]₂[ReBr₃(CO)₃] (0.076 g, 0.099 mmol) and L¹ (0.040 g, 0.099 mmol) in MeOH (10 mL) was heated to reflux for 6 h. The solvent was removed in vacuo, and the residue was purified by alumina (Brockman activity I, neutral) chromatography (8.5:1.5 CH₃CN:H₂O eluent) to afford the product as a white solid (0.035 g, 46%). ¹H NMR (MeOH-*d*₄, 400.13 MHz): δ 8.89 (d, ³J_{13,14} = 5.3 Hz, 2H; H-14), 7.96 (dd, ³J_{11,12} = 7.3 Hz, ³J_{12,13} = 8.0 Hz, 2H; H-12),

7.60 (d, ³J_{11,12} = 7.3 Hz, 1H; H-11), 7.59 (d, ³J_{11,12} = 7.3 Hz, 1H; H-11') 7.39 (dd, ³J_{12,13} = 8.0 Hz, ³J_{13,14} = 5.3 Hz, 2H; H-13), 5.11 (overlapping d, ²J_{9a,9b/9'a,9'b} = 16.8 Hz, 2H; H-9a, H-9'a), 4.99 (overlapping d, ²J_{9a,9b/9'a,9'b} = 16.8 Hz, 2H; H-9b, H-9'b), 4.49 (d, ³J_{1,2} = 7.8 Hz, 1H; H-1), 4.45 (m, 1H; H-7a), 4.20 (m, 2H; 2x H-8), 4.12 (m, 1H; H-7b), 3.87 (dd, ³J_{5,6a} = 1.5 Hz, ²J_{6a,6b} = 11.7 Hz, 1H; H-6a), 3.76 (dd, ³J_{5,6b} = 5.2 Hz, ²J_{6a,6b} = 11.7 Hz, 1H; H-6b), 3.30–3.49 (m, 4H; H-2, H-3, H-4, H-5). ¹³C{¹H} NMR (MeOH-*d*₄, 100.62 MHz): δ 197.22, 196.36 [*fac*-Re(CO)₃], 162.53 (C10), 162.51 (C10'), 153.02 (C14), 141.61 (C12), 126.84 (C11), 124.70 (C13), 124.66 (C13'), 104.59 (C1), 78.16, 78.08 (C3/C5), 75.03 (C2), 71.57 (C4), 70.77 (C8), 69.48, 69.45 (C9/C9'), 67.49 (C7), 62.61 (C6). IR (cm⁻¹, thin film, AgBr plate): 3379 (br) [ν(OH)]; 2930 (w) [ν(CH)]; 2027 (vs), 1931 (vs) [ν(*fac*-Re(CO)₃)]; 1611 (w) [ν(C=C or C=N)]. ES-MS *m/z* (relative intensity) = 676, 674 ([M]⁺, 100). Λ_M = 165 Ω⁻¹ cm² mol⁻¹ (1:1 electrolyte). Anal. Calcd (found) for C₂₃H₂₇N₃O₉ReBr·2H₂O: C, 34.90 (35.17); H, 3.95 (3.76); N, 5.31 (5.20).

(2-Bis(2-pyridinylmethyl)amino)ethyl-β-D-xylopyranosyl)-tricarboxylrhodium bromide [Re(L²)(CO)₃]Br. The title compound [Re(L²)(CO)₃]Br (0.087 g, 75%) was prepared from [NEt₄]₂[ReBr₃(CO)₃] (0.108 g, 0.141 mmol) and L² (0.053 g, 0.141 mmol) by a procedure analogous to that described for [Re(L¹)(CO)₃]Br. ¹H NMR (MeOH-*d*₄, 400.13 MHz): δ 8.89 (d, ³J_{13,14} = 5.6 Hz, 2H; H-14), 7.98 (dd, ³J_{11,12} = 7.6 Hz, ³J_{12,13} = 8.0 Hz, 2H; H-12), 7.67 (d, ³J_{11,12} = 7.6 Hz, 1H; H-11), 7.65 (d, ³J_{11,12} = 7.6 Hz, 1H; H-11'), 7.41 (dd, ³J_{12,13} = 8.0 Hz, ³J_{13,14} = 5.6 Hz, 2H; H-13), 5.07 (overlapping d, ²J_{9a,9b/9'a,9'b} = 16.7 Hz, 2H; H-9a, H-9'a), 5.01 (d, ²J_{9a,9b} = 16.7 Hz, 1H; H-9b), 4.99 (d, ²J_{9'a,9'b} = 16.7 Hz, 1H; H-9'b), 4.45 (d, ³J_{1,2} = 7.6 Hz, 1H; H-1), 4.36 (m, 1H; H-7a), 4.19 (m, 2H; 2x H-8), 4.13 (m, 1H; H-7b), 3.96 (dd, ³J_{4,5a} = 5.3 Hz, ²J_{5a,5b} = 11.4 Hz, 1H; H-5a), 3.56 (ddd, ³J_{3,4} = 10.2 Hz, ³J_{4,5a} = 5.3 Hz, ³J_{4,5b} = 8.8 Hz, 1H; H-4), 3.42 (dd, ³J_{2,3} = 8.7 Hz, ³J_{3,4} = 10.2 Hz, 1H; H-3), 3.33 (m, 2H; H-2, H-5b). ¹³C{¹H} NMR (MeOH-*d*₄, 100.62 MHz): δ 197.18, 196.33 [*fac*-Re(CO)₃], 162.46 (C10), 162.37 (C10'), 153.06 (C14), 153.03 (C14'), 141.63 (C12), 141.61 (C12'), 126.87 (C11), 126.86 (C11'), 124.72 (C13), 124.69 (C13'), 105.34 (C1), 77.90 (C3), 74.87 (C2), 71.15 (C4), 70.62 (C8), 69.70, 69.34 (C9, C9'), 67.63 (C7), 67.15 (C5). IR (cm⁻¹, thin film, AgBr plate): 3378 (br) [ν(OH)]; 2935 [ν(CH)]; 2029 (vs), 1920 (vs) [ν(*fac*-Re(CO)₃)]; 1611 (w) [ν(C=C or C=N)]. ES-MS *m/z* (relative intensity) = 646, 644 ([M]⁺, 100). Λ_M = 141 Ω⁻¹ cm² mol⁻¹ (1:1 electrolyte). Anal. Calcd (found) for C₂₂H₂₅N₃O₈ReBr·3H₂O: C, 33.89 (33.83); H, 4.01 (3.97); N, 5.39 (5.78).

(2-Bis(2-pyridinylmethyl)amino)ethyl-α-D-mannopyranosyl)-tricarboxylrhodium bromide [Re(L³)(CO)₃]Br. The title compound [Re(L³)(CO)₃]Br (0.064 g, 63%) was prepared from [NEt₄]₂[ReBr₃(CO)₃] (0.105 g, 0.136 mmol) and L³ (0.055 g, 0.136 mmol) by a procedure analogous to that described for [Re(L¹)(CO)₃]Br. ¹H NMR (MeOH-*d*₄, 400.13 MHz): δ 8.89 (d, ³J_{13,14} = 5.5 Hz, 2H; H-14), 7.98 (dd, ³J_{11,12} = 7.6 Hz, ³J_{12,13} = 7.8 Hz, 2H; H-12), 7.62 (d, ³J_{11,12} = 7.6 Hz, 1H; H-11), 7.60 (d, ³J_{11,12} = 7.6 Hz, 1H; H-11'), 7.39 (dd, ³J_{12,13} = 7.8 Hz, ³J_{13,14} = 5.5 Hz, 2H; H-13), 5.07 (overlapping d, ²J_{9a,9b/9'a,9'b} = 16.8 Hz, 2H; H-9a, H-9'a), 4.99 (d, ²J_{9a,9b} = 16.8 Hz, 1H; H-9b), 4.98 (d, ³J_{1,2} = 1.3 Hz, 1H; H-1), 4.97 (d, ²J_{9'a,9'b} = 16.8 Hz, 1H; H-9'b), 4.28 (m, 1H; H-7a), 4.17 (m, 2H; 2x H-8), 4.04 (m, 2H; H-2, H-7b), 3.96 (dd, ³J_{5,6a} = 1.6 Hz, ²J_{6a,6b} = 11.0 Hz, 1H; H-6a), 3.80 (m, 2H; H-3, H-6b), 3.68 (m, 2H; H-4, H-5). ¹³C{¹H} NMR (MeOH-*d*₄, 100.62 MHz): δ 197.17, 196.29 [*fac*-Re(CO)₃], 162.26 (C10), 162.23 (C10'), 153.05 (C14), 141.61 (C12), 126.92 (C11), 126.90 (C11'), 124.83 (C13), 124.81 (C13'), 102.15 (C1), 75.45 (C4/C5), 72.57 (C3), 71.86 (C2), 70.41 (C8), 69.66, 69.30 (C9, C9'), 68.61 (C4/C5), 65.52 (C7),

(34) SAINT, version 6.02; Bruker AXS Inc.: Madison, WI, 1999.

(35) SADABS, version 2.05; Bruker AXS Inc.: Madison, WI, 1999.

(36) Altomare, A.; Cascarano, M.; Giacovazzo, C.; Guagliardi, A.; SIR92. *J. Appl. Crystallogr.* **1994**, *26*, 343.

(37) SHELXL, version 5.1; Bruker AXS Inc.: Madison, WI, 1997.

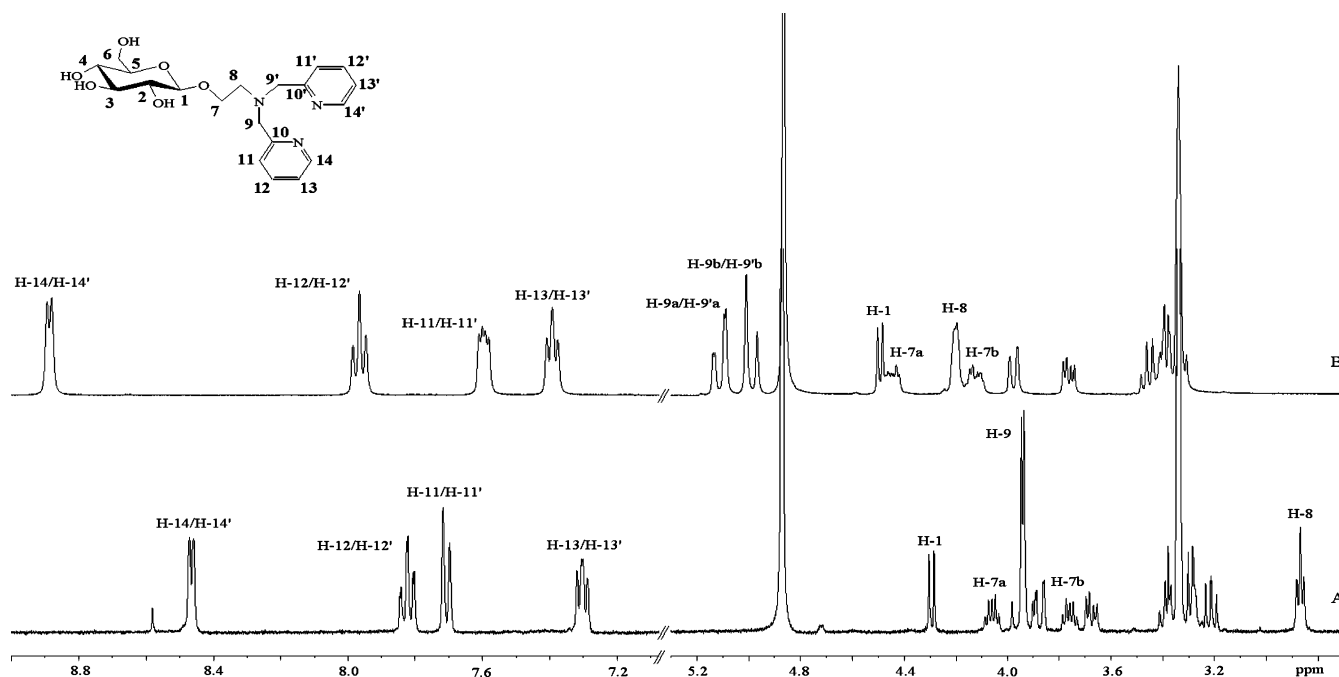
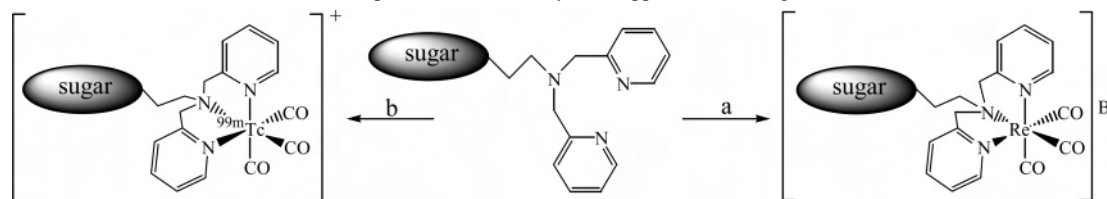


Figure 1. ^1H NMR (MeOH- d_4 , 400 MHz) of (A) L^1 and (B) $[\text{Re}(\text{L}^1)(\text{CO})_3]\text{Br}$.

Scheme 1. Reaction Scheme for Re and $^{99\text{m}}\text{Tc}$ Complexes of the Carbohydrate-Appended DPA Ligands $\text{L}^1\text{--L}^3$ ^a



^a Key: (a) $[\text{NEt}_4]_2[\text{ReBr}_3(\text{CO})_3]$, MeOH, 6 h, 46–75% yield; (b) $[\text{}^{99\text{m}}\text{Tc}(\text{H}_2\text{O})_3(\text{CO})_3]^+$, 70 °C, 40 min, PBS buffer.

62.98 (C6). IR (cm^{-1} , thin film, AgBr plate): 3389 (br) [$\nu(\text{OH})$]; 2935 [$\nu(\text{CH})$]; 2027 (vs), 1932 (vs) [$\nu(\text{fac-Re}(\text{CO})_3)$]; 1611 (w) [$\nu(\text{C}=\text{C}$ or $\text{C}=\text{N})$]. ES-MS m/z (relative intensity) = 676, 674 ($[\text{M}]^+$, 100). $\Lambda_{\text{M}} = 160 \Omega^{-1} \text{cm}^2 \text{mol}^{-1}$ (1:1 electrolyte). Anal. Calcd (found) for $\text{C}_{23}\text{H}_{27}\text{N}_3\text{O}_9\text{ReBr}\cdot 2\text{H}_2\text{O}$: C, 34.90 (34.77); H, 3.95 (3.65); N, 5.31 (5.59).

Results and Discussion

Synthesis and Spectroscopic Properties. The synthesis of the Re complexes proceeded in a straightforward manner from $[\text{NEt}_4]_2[\text{ReBr}_3(\text{CO})_3]$ and one of $\text{L}^1\text{--L}^3$ in refluxing methanol to afford the compounds $[\text{Re}(\text{L}^{1-3})(\text{CO})_3]\text{Br}$ in moderate yield after chromatography (Scheme 1). ^1H NMR analysis of the crude product was consistent in each case with the quantitative formation of the proposed structures as well as the presence of the byproduct NEt_4Br . This salt was then removed by column chromatography to afford the complexes as hygroscopic white powders stable in the solid

state and in aqueous solution. The identity of the compounds was probed in solution via conductivity measurements. The Re compounds (1 mM) were dissolved in deionized water, and the conductivity was measured and compared to a number of 1:1 electrolyte solutions ($\text{NaCl} = 125 \Omega^{-1} \text{cm}^2 \text{mol}^{-1}$, $[\text{NBu}_4]\text{Br} = 113 \Omega^{-1} \text{cm}^2 \text{mol}^{-1}$, $[\text{MePPh}_3]\text{Br} = 108 \Omega^{-1} \text{cm}^2 \text{mol}^{-1}$). As expected, the conductivity values for the Re compounds correspond to 1:1 electrolytes³³ at the concentrations measured (Table 2).

NMR analysis of the Re compounds in MeOH- d_4 was indicative of the mode of ligand binding (N-atoms) and illustrated the lower symmetry of the ligands once bound to the $\{\text{Re}(\text{CO})_3\}^+$ core. Due to the electronic influence of the Re(I) center, a significant downfield shift of the hydrogen resonances in close proximity to the ligating N-atoms was observed. The pyridine hydrogens H-14/H-14' (Figure 1) move downfield by approximately 0.5 ppm, while the

Table 2. HPLC Retention Times (RT), Labeling Yields (%), and Conductivity Measurements for the $[\text{M}(\text{L}^1\text{--L}^3)(\text{CO})_3]^+$ (M = Re, $^{99\text{m}}\text{Tc}$) Complexes

complex $[\text{M}(\text{L})(\text{CO})_3]^+$	RT (min) M = Re (254 nm)	RT (min) M = $^{99\text{m}}\text{Tc}$ (radiometric)	labeling yield (%) \pm SD ($n=3$)	conductivity (M = Re) (H_2O) Λ_{m} ($\Omega^{-1} \text{cm}^2 \text{mol}^{-1}$)
L^1	13.8	13.7	99 \pm 1	165
L^2	14.5	14.6	99 \pm 1	141
L^3	13.7	13.9	99 \pm 1	160
$[\text{M}(\text{His})(\text{CO})_3]$		12.2		
$[\text{M}(\text{H}_2\text{O})_3(\text{CO})_3]^+$		13.0		

hydrogens of the ethylene linker (H-8) adjacent to the tertiary amine shift downfield by 1.5 ppm upon ligand binding. As well, the hydrogen signals of the methylene groups (H-9a/H-9b and H-9'a/H-9'b) adjacent to the pyridine rings shifted downfield (~ 1.1 ppm) and become diastereotopic exhibiting geminal coupling (~ 17 Hz).

The hydrogen and carbon resonances of the sugar moieties were either unchanged or exhibited very minor shifts as compared to those in the free ligands. Coordination-induced shifts^{38,39} (CIS) would suggest carbohydrate ligation to the metal center. The lack of these shifts confirms the pendant nature of the carbohydrate functions in solution. The carbohydrate moieties do however exert a long-range asymmetric effect on the compounds described herein. This asymmetric effect is present in the ^1H NMR spectrum of the ligands as hydrogens H-7a/H-7b are diastereotopic (Figure 1A). However, the effect of the carbohydrate is extended upon binding to the $\{\text{Re}(\text{CO})_3\}^+$ core, most likely due to the conformational restriction of the ligand upon chelation. The two methylene carbons (9/9'), adjacent to the pyridines, exhibit separate ^{13}C signals in all three Re complexes. As well, a complicated pattern arises for the diastereotopic methylene hydrogen signals (H-9a/H-9b and H-9'a/H-9'b). The observed pattern can be explained by the fact that the four hydrogens are essentially nonidentical. The effect is more pronounced (due to larger chemical shift differences) for the xylose and mannose derivatives in the ^1H NMR spectrum. Long-range ^1H – ^1H COSY measurements highlight the weak coupling (~ 1 – 2 Hz) between H-11/H-11' and the hydrogens of the methylene groups (H-9a/H-9b and H-9'a/H-9'b), leading to further broadening of the latter hydrogen signals. The pyridine rings also display inequivalency by NMR. The pattern displayed by H-11/H-11' changes substantially upon metal binding (Figure 1) with two distinct doublets evident. The pyridine carbons also exhibit two signals in the ^{13}C spectra of the Re complexes. It is intriguing that the pendant carbohydrate moiety exerts an effect as distant as the pyridine rings. Interestingly, the ^{13}C data of the complexes reveal that there are only two Re–CO peaks in a 2:1 peak height ratio. This result can be explained by (a) simple overlap or (b) that two of the CO groups are magnetically equivalent because of the mirror symmetry along the axis formed by the Re with one CO group. The latter argument is mostly obviated by the NMR results already discussed.

The IR spectra of the Re compounds were consistent with the proposed structures; bands attributable to the $\{\text{Re}(\text{CO})_3\}^+$ core were present between 2100 and 1800 cm^{-1} .^{25,31} In each of the three metal complexes, two CO bands were present. The broader, lower band $\sim 1930\text{ cm}^{-1}$ is most probably due to the overlap of two CO absorptions based on symmetry considerations.

The Re compounds were further examined by mass spectrometry. Re exists as a mixture of $^{185}\text{Re}/^{187}\text{Re}$ isotopes

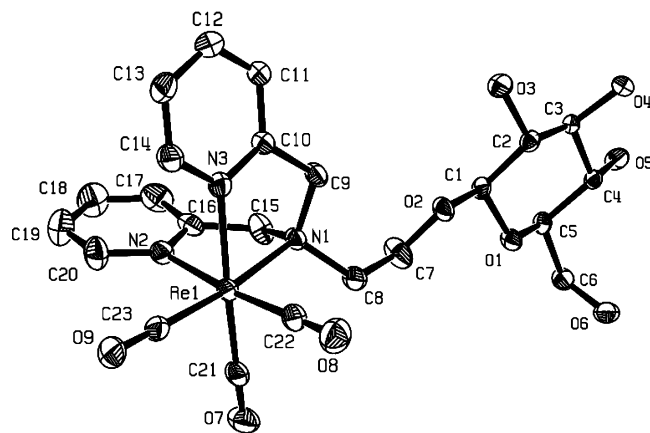


Figure 2. ORTEP view of the structure of the cation $[\text{Re}(\text{L}^1)(\text{CO})_3]^+$ showing the atom labeling scheme (50% thermal ellipsoids).

(37.4% and 62.6% abundance, respectively) affording diagnostic peak isotope patterns. The compounds were run as dilute solutions in MeOH and displayed the molecular ion $[\text{M}]^+$ peak in 100% abundance for the three complexes. For the glucose and mannose derivatives, the peak centered at m/z 675 is assigned to $[\text{Re}(\text{L}^{1,3})(\text{CO})_3]^+$. For the xylose derivative, the peak centered at m/z 645 corresponds to $[\text{Re}(\text{L}^2)(\text{CO})_3]^+$. In all cases the theoretical isotope patterns matched the experimental spectra.

Crystallographic Studies. One of the Re compounds, $[\text{Re}(\text{L}^1)(\text{CO})_3]\text{Cl}$, was crystallized as the chloride salt and analyzed by X-ray crystallography. These data are only the third report of a Re organometallic carbohydrate structure.⁴ A manganese dicarbonyl(carbohydratocarbene) complex⁴⁰ is the only other group VII organometallic carbohydrate X-ray structure that has been described. Structures of oxorhenium(V) complexes with carbohydrate moieties directly bound to the metal center have also been reported,³⁹ using hydridotris(pyrazolyl)borato as the ancillary tridentate ligand. Very few carbohydrate-containing transition metal complexes in which the carbohydrate moiety is not only unprotected but also unbound to the metal center have been crystallized.^{4,13,41}

The molecular structure of the cation $[\text{Re}(\text{L}^1)(\text{CO})_3]^+$ and the atomic labeling scheme are presented in Figure 2 with the relevant bond lengths and angles collected in Table 3. The structure consists of discrete Cl^- anions, $[\text{Re}(\text{L}^1)(\text{CO})_3]^+$ cations, and solvent ($\text{Et}_2\text{O}/\text{MeOH}$) in the lattice. A salient feature of this structure is the pendant carbohydrate (glucose) in accordance with the solution characterization data. The distorted octahedral environment of Re(I) is occupied by three facially arranged carbonyls and the amine and pyridyl nitrogen donors of the ligand. The facial arrangement of the ligand, imposed by the $\{\text{Re}(\text{CO})_3\}^+$ core, is in contrast to the meridional binding seen in a Cu(II) complex of the same ligand,³⁰ highlighting the versatility of the DPA function for

(38) (a) Klufers, P.; Kunte, T. *Chem. Eur. J.* **2003**, *9*, 2013–2018. (b) Klufers, P.; Kunte, T. *Angew. Chem., Int. Ed.* **2001**, *40*, 4210–4212.

(39) Klufers, P.; Krotz, O.; Ossberger, M. *Eur. J. Inorg. Chem.* **2002**, 1919–1923.

(40) Fischer, H.; Weissenbach, K.; Karl, C.; Geyer, A. *Eur. J. Inorg. Chem.* **1998**, 339–347.

(41) (a) Brudzinska, I.; Mikata, Y.; Obata, M.; Ohtsuki, C.; Yano, S. *Bioorg. Med. Chem. Lett.* **2004**, *14*, 2533–2536. (b) Yano, S.; Shinohara, Y.; Mogami, K.; Yokoyama, M.; Tanase, T.; Sakakibara, T.; Nishida, F.; Mochida, K.; Kinoshita, I.; Doe, M.; Ichihara, K.; Naruta, Y.; Mehrkhodavandi, P.; Buglyo, P.; Song, B.; Orvig, C.; Mikata, Y. *Chem. Lett.* **1999**, 255–256.

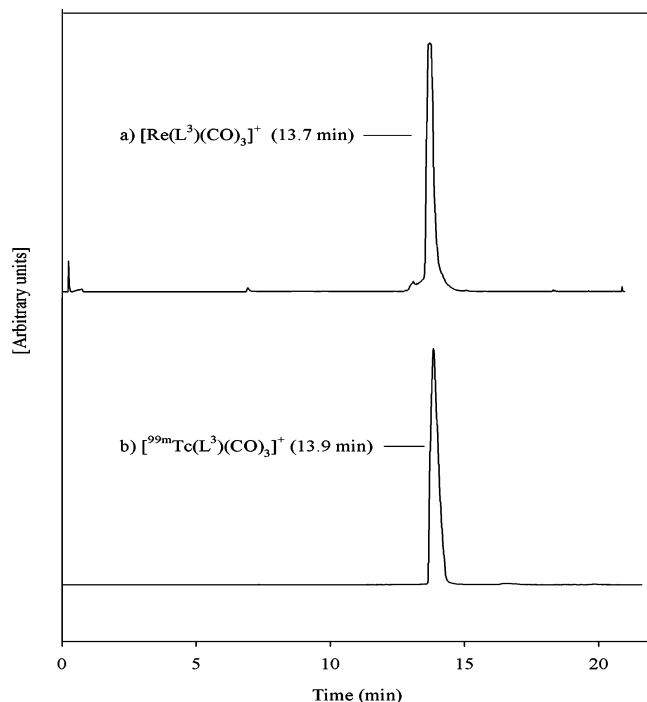


Figure 3. HPLC comparison of (a) $[\text{Re}(\text{L}^3)(\text{CO})_3]^+$ (UV/254 nm) and (b) $[\text{}^{99\text{m}}\text{Tc}(\text{L}^3)(\text{CO})_3]^+$ (radiometric).

Table 3. Selected Bond Lengths (Å) and Angles (deg) in $[\text{Re}(\text{L}^1)(\text{CO})_3]\text{Cl}$

Re(1)–N(1)	2.227(3)	N(1)–Re(1)–N(2)	78.42(10)
Re(1)–N(2)	2.167(3)	N(1)–Re(1)–N(3)	77.66(10)
Re(1)–N(3)	2.177(3)	N(2)–Re(1)–N(3)	80.58(10)
Re(1)–C(21)	1.930(4)	N(1)–Re(1)–C(21)	94.25(12)
Re(1)–C(22)	1.926(4)	N(1)–Re(1)–C(22)	97.65(12)
Re(1)–C(23)	1.918(3)	N(1)–Re(1)–C(23)	173.25(12)
C(22)–O(8)	1.154(8)	C(21)–Re(1)–C(22)	90.10(15)
		C(21)–Re(1)–C(23)	89.74(14)

metal ion chelation. The Re–CO distances (1.918–1.930 Å) are analogous to those found in similar complexes.^{25,42} The Re(1)–N(1) distance [2.227(3) Å] is slightly longer than the Re–pyridine(N) distances [Re(1)–N(2) 2.167(3) Å, Re(1)–N(3) 2.177(3)] consistent with the hybridization of the N-donors (sp^3 vs sp^2). The most significant distortion in the structure are the angles $\text{N}(1)\text{--Re}(1)\text{--N}(2) = 78.42(10)^\circ$ and $\text{N}(1)\text{--Re}(1)\text{--N}(3) = 77.66(10)^\circ$ due to the formation of strained five-membered chelate rings. Finally, the glucose moiety exists exclusively as the β -anomer in the solid-state structure, correlating well with solution NMR data.

In Vitro Characterization and Stability of the $^{99\text{m}}\text{Tc}$ -Labeled Carbohydrates. The $^{99\text{m}}\text{Tc}$ -labeled carbohydrate compounds were synthesized utilizing a previously established method.^{24,43} The formation of the $[\text{}^{99\text{m}}\text{Tc}(\text{H}_2\text{O})_3(\text{CO})_3]^+$ precursor was verified by HPLC (RT = 13.0 min, Table 2) before labeling with the carbohydrate ligands $\text{L}^1\text{--L}^3$. The labeled derivatives were then characterized by their associated radioactive HPLC traces and compared, via co-injection, with the corresponding Re complexes (monitored at 254 nm). In all cases the retention times of the Re and $^{99\text{m}}\text{Tc}$ complexes

were identical within experimental error (Table 2 and Figure 1). Figure 3 compares the HPLC traces of the Re and $^{99\text{m}}\text{Tc}$ complexes of L^3 . These results confirm that the complexes produced on the tracer level are identical to Re complexes produced and characterized (vide supra) on the macroscopic scale. The labeling yields for the three compounds were essentially quantitative under the conditions studied, and the yields shown in Table 2 are the average of at least three separate experiments.

The in vitro stability of the $^{99\text{m}}\text{Tc}$ complexes was assessed by incubation with solutions of either cysteine or histidine.²⁴ The susceptibility of the complexes to ligand exchange by these amino acids was assessed over a 24-h period. One recent study using the DPA framework for ligating to the $\{\text{}^{99\text{m}}\text{Tc}(\text{CO})_3\}$ core demonstrated the exceptional stability of the resulting complex toward ligand exchange in solutions of histidine or human serum.²⁸ The tridentate DPA ligands were thus expected to form stable complexes resistant to ligand exchange processes, and this was indeed the case; no decomposition occurred upon incubation of $[\text{}^{99\text{m}}\text{Tc}(\text{L}^1)(\text{CO})_3]^+$ with an excess (10-fold) of either cysteine or histidine over a 24-h period (data not shown). This is in contrast to our recent report of $^{99\text{m}}\text{Tc}$ complexes with a series of bidentate carbohydrate-appended ligands that exhibited decomposition at the 24-h time point in the presence of excess histidine.⁴ This decomposition is most likely due to the substitution of the coordinated water molecule by the functional groups of histidine leading to subsequent displacement of the carbohydrate ligands. To better examine the stability of the complexes reported herein, the stability studies were run with a 100-fold excess of either cysteine or histidine. Even at higher amino acid concentrations the $^{99\text{m}}\text{Tc}$ complexes were $\geq 95\%$ intact at the 24-h time point. Clearly matching the tridentate binding capability of these ligands to the *fac*- $\{\text{M}(\text{CO})_3\}^+$ core greatly stabilizes the resulting complexes to ligand substitution processes in vitro and hopefully in vivo as well.

Concluding Remarks

In this work, we have described the synthesis, resultant solution, and solid-state properties of a series of carbohydrate-appended DPA ligands bound to the $\{\text{M}(\text{CO})_3\}^+$ ($\text{M} = \text{}^{99\text{m}}\text{Tc}/\text{Re}$) core. The pendant nature of the carbohydrate groups was confirmed for the Re compounds in solution by NMR as well as in the solid state by X-ray crystallography. Radio-labeling of the carbohydrate-appended DPA ligands using the labeling precursor $[\text{}^{99\text{m}}\text{Tc}(\text{H}_2\text{O})_3(\text{CO})_3]^+$ was essentially quantitative and afforded compounds identical to the Re analogues on the basis of HPLC comparison. The radio-labeled compounds were determined to be stable to ligand exchange in the presence of an excess of either cysteine or histidine over a 24-h period. On the basis of these promising results, we are planning to evaluate the biodistribution of the $^{99\text{m}}\text{Tc}$ complexes in suitable model systems. In addition, labeling studies of the carbohydrate ligands with the therapeutic isotope ^{186}Re are underway.

Acknowledgment. The authors gratefully acknowledge the Natural Sciences and Engineering Research Council

(42) Reger, D. L.; Gardinier, J. R.; Pellechia, P. J.; Smith, M. D.; Brown, K. J. *Inorg. Chem.* **2003**, *42*, 7635–7643.

(43) Alberto, R.; Schibli, R.; Egli, A.; Schubiger, A. P.; Abram, U.; Kaden, T. A. *J. Am. Chem. Soc.* **1998**, *120*, 7987–7988.

Carbohydrate-Appended ^{99m}Tc and Re Complexes

(NSERC) of Canada for a Strategic grant and the Ministry of Education, Culture, Sports, Science, and Technology (MEXT) of Japan for a Grant-in-Aid for Scientific Research (Nos. 15750144, 16350032, and 13557211). T.S. acknowledges NSERC for a postgraduate scholarship as well as the Japanese Society for the Promotion of Science (JSPS) for a travel award. Mallinckrodt Inc. is acknowledged for the Isolink boranocarbonate kits, and the UBC Hospital Department of Nuclear Medicine is acknowledged for supplying

$[\text{}^{99m}\text{TcO}_4]^-$. Dr. B. O. Patrick is acknowledged for assistance with the X-ray determination, as is UBC for a University Graduate Fellowship (C.A.B.).

Supporting Information Available: X-ray crystallographic file in CIF format for the structure of $[\text{Re}(\text{L}^1)(\text{CO})_3]\text{Cl}$. This material is available free of charge via the Internet at <http://pubs.acs.org>.

IC048528I